

August, 31 2020

Lepton-pair production in hard exclusive hadron-hadron collisions

S.V. Goloskokov ^{§1}, P. Kroll ^{†2} and O. Teryaev ^{§‡3}

§: *Bogoliubov Laboratory of Theoretical Physics, Joint Institute for Nuclear Research, Dubna 141980, Moscow region, Russia*

†: *Fachbereich Physik, Universität Wuppertal, D-42097 Wuppertal, Germany*

‡: *Veksler and Baldin Laboratory of High Energy Physics, Dubna 141980, Moscow region, Russia*

Abstract

We investigate lepton-pair production in hard exclusive hadron-hadron collisions. We consider a double handbag (DH) mechanism in which the process amplitude factorizes in hard subprocesses, $qq \rightarrow qq\gamma^*$ and $qq \rightarrow qg\gamma^*$, and in soft hadron matrix elements parameterized as generalized parton distributions (GPDs). Employing GPDs extracted from exclusive meson electroproduction, we present predictions for the lepton-pair cross section at kinematics typical for the LHC, NICA and FAIR. It turns out from our numerical studies that the quark-gluon subprocess dominates by far, the quark-quark(antiquark) subprocesses are almost negligible.

1 Introduction

In the last two decades there were a lot of activities in the measurement and the theoretical analysis of hard exclusive processes, such as deeply virtual Compton scattering or electroproduction of mesons. The theoretical analyses of these processes, beginning with the pioneering articles by Ji [1] and Radyushkin [2], bases on factorization of the process amplitudes in hard, perturbatively calculable parton-level subprocesses and in soft hadronic matrix elements, parameterized as general parton distributions (GPDs). This type of factorization, often dubbed as the handbag approach, has been shown to hold for the mentioned processes [3, 4] in the generalized Bjorken regime of large photon virtuality, Q^2 , and large center-of-mass energy at fixed Bjorken- x and small squared invariant momentum transfer, t ($-t \ll Q^2$). This type of factorization has also been applied to wide-angle processes, e.g. [5, 6], and time-like ones, e.g. [7]. In contrast to the deeply virtual processes, rigorous proofs of factorization do

¹Email: goloskkv@theor.jinr.ru

²Email: kroll@physik.uni-wuppertal.de

³Email: teryaev@jinr.ru

not exist for the latter processes. Experimental and theoretical investigations, however, revealed that for moderately large photon virtualities there are frequently substantial corrections to the asymptotic handbag picture, e.g. in π^0 electroproduction [8, 9].

In the present paper we are interested in lepton-pair production in hard exclusive hadronic collisions

$$A B \rightarrow A B l^+ l^- \quad (1)$$

at large Mandelstam s and large, time-like photon virtualities but small momentum transfer. This exclusive analogue of the Drell-Yan process can, in principle, be measured at the LHC and at the future accelerators NICA, FAIR and J-PARC. We assume the above described factorization in hard parton-level subprocesses and in soft proton matrix elements to hold and describe the process (1) by a double handbag, see Fig. 1. The double handbag is also appearing due to analytic properties of the relevant amplitude [10]). The DH mechanism has already been applied to exclusive reactions involving charmed hadrons such as $p\bar{p} \rightarrow \Lambda_c \bar{\Lambda}_c$ [11] or $\pi^- p \rightarrow D^- \Lambda_c^+$ [12]. In these reactions the large scale is set by the mass of the charm quark. An alternative dynamical mechanism to the double handbag is depicted on the right-hand side of Fig. 1: A photon is emitted from one of the hadrons and interacts with a constituent quark from the other hadron in the sense of time-like virtual Compton scattering (TVCS). This process has been studied theoretically, e.g. in [13, 14] but has not yet been measured. We expect that this single-handbag mechanism leads to much smaller cross sections than the double handbag except perhaps in ultraperipheral heavy ion reactions. The strong quark-gluon subprocesses contributing only to the double handbag will dominate as we are going to demonstrate in the following sections. The single-handbag mechanism has been advocated for by Cisek et al [15] for the production of heavy vector mesons, like the J/Ψ , in semiexclusive hadron-hadron and hadron-nucleus collisions. Of course, the purely electromagnetic lepton-pair production is also to be considered by us.

The plan of the paper is as follows: A kinematical prelude is presented in the next section and, in Sect. 3, the hard subprocesses are described in some detail. The full $A B \rightarrow A B l^+ l^-$ amplitudes, given as convolutions of the subprocess amplitudes and GPDs, are discussed in Sect. 4. In the following section the purely electromagnetic generation of lepton pairs in exclusive hadronic collisions is discussed. The DH amplitudes, derived in Sect. 4, are specified for particular processes in Sect. 6 and some numerical results for cross sections are given. We also discuss the relative strength of the electromagnetic and DH contributions in this section. In the Appendix some useful formulas for the phase space and the decay of the virtual photon are repeated.

2 Kinematics

First we consider the process $A(p_a, \mu_a) B(p_b, \mu_b) \rightarrow A(q_1, \mu_1) B(q_2, \mu_2) \gamma^*(q_3, \nu)$ where A and B are protons, antiprotons or pions. The decay of the virtual photon into the lepton pair will be treated separately in App. A. The momenta and helicities of the various particles are denoted by p_i, q_i and μ_a, \dots, μ_2 and

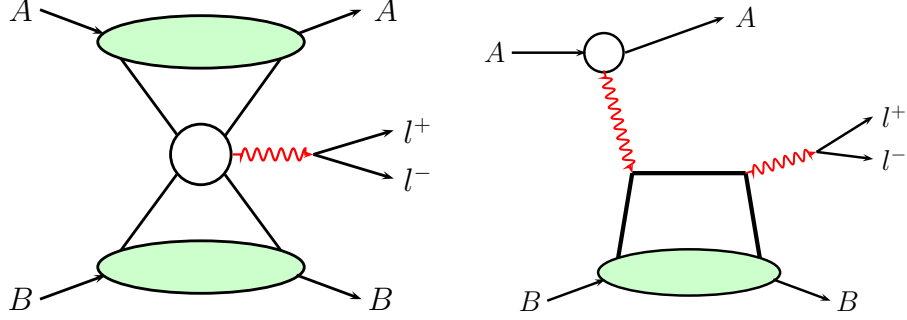


Figure 1: Left: The double handbag for exclusive lepton-pair production in hadron-hadron collisions. Right: The TVCS mechanism.

ν , respectively. Since we assume large s the hadron masses will be neglected throughout the paper. Momentum conservation tells us that

$$p_a + p_b = q_1 + q_2 + q_3. \quad (2)$$

It is convenient to introduce the following Lorentz invariants in addition to $s = (p_a + p_b)^2$

$$\begin{aligned} s_1 &= (q_1 + q_3)^2, & s_2 &= (q_2 + q_3)^2, \\ t_1 &= (p_a - q_1)^2, & t_2 &= (p_b - q_2)^2. \end{aligned} \quad (3)$$

The following relations hold [16]

$$\begin{aligned} s_1 + t_1 - t_2 &= 2p_a \cdot q_3, \\ s_2 + t_2 - t_1 &= 2p_b \cdot q_3, \end{aligned} \quad (4)$$

and, in the limit $t_1, t_2 \rightarrow 0$,

$$s_1 \simeq s_2 \simeq \sqrt{s}Q. \quad (5)$$

The hadron momenta, given in light-cone coordinates, are parameterized in Ji's frame [17] by:

$$\begin{aligned} p_a &= \left[(1 + \xi_1)\bar{p}_a^+, \frac{\Delta_{1\perp}^2}{8(1 + \xi_1)\bar{p}_a^+}, -\frac{1}{2}\Delta_{1\perp}, 0 \right], \\ p_b &= \left[\frac{\Delta_{1\perp}^2}{8(1 + \xi_2)\bar{p}_b^-}, (1 + \xi_2)\bar{p}_b^-, \frac{1}{2}\Delta_{1\perp}, 0 \right], \\ q_1 &= \left[(1 - \xi_1)\bar{p}_a^+, \frac{\Delta_{1\perp}^2}{8(1 - \xi_1)\bar{p}_a^+}, \frac{1}{2}\Delta_{1\perp}, 0 \right], \\ q_2 &= \left[\frac{\Delta_{2\perp}^2}{8(1 - \xi_2)\bar{p}_b^-}, (1 - \xi_2)\bar{p}_b^-, -\frac{1}{2}\Delta_{2\perp} \cos \Phi_2, -\frac{1}{2}\Delta_{2\perp} \sin \Phi_2 \right], \end{aligned} \quad (6)$$

where \bar{p}_a^+ (\bar{p}_b^-) is the plus (minus) component of the average hadron momentum $\bar{p}_a = (p_a + q_1)/2$ ($\bar{p}_b = (p_b + q_2)/2$) at the upper (lower) hadronic blob of the graph shown on the left-hand side of Fig. 1. As usual the skewness parameter,

ξ_1 (ξ_2), represents the ratio of the plus (minus) components of the difference and the sum of the hadron momenta at the upper (lower) blob. The skewness parameters as well as \bar{p}_a^+ and \bar{p}_b^- can be expressed in terms of the invariants. Up to corrections of order t_i/Q^2 ($i = 1, 2$), the expressions read

$$\begin{aligned}\bar{p}_a^+ &= \frac{2s - s_2}{2\sqrt{2s}}, & \bar{p}_b^- &= \frac{\sqrt{s}}{2\sqrt{2}} \frac{4s - 2s_1 - 2s_2 + Q^2}{2s - s_2}, \\ \xi_1 &= \frac{s_2}{2s - s_2}, & \xi_2 &= \frac{2s_1 - Q^2}{4s - 2s_1 - 2s_2 + Q^2}.\end{aligned}\quad (7)$$

Working in that frame means that we have to use the GPDs according to Ji's definition [17]. These GPDs are invariant under boosts in the 3-direction and under rotations around the 3-axis but are not invariant, for instance, under rotations around the 2-axis.

In Ji's frame the Mandelstam t_i are related to the momentum transfers, $\Delta_{i\perp}$, by

$$\begin{aligned}t_1 &= -\frac{\Delta_{1\perp}^2}{1 - \xi_1^2}, \\ t_2 &= -\frac{1}{4} \frac{\left[(1 - \xi_2)\Delta_{1\perp} - (1 + \xi_2)\Delta_{2\perp}\right]^2}{1 - \xi_2^2} - \Delta_{1\perp}\Delta_{2\perp} \sin^2(\Phi_2/2).\end{aligned}\quad (8)$$

Thus, the limits $t_i \rightarrow 0$ imply $\Delta_{i\perp} \rightarrow 0$.

3 The subprocess amplitudes

As already mentioned we are interested in the process $AB \rightarrow AB\gamma^*$ at large s , large photon virtuality, $q_3^2 = Q^2$, but small momentum transfer at the hadronic vertices, $t_i \ll Q^2$ ($i = 1, 2$). According to the handbag factorization it is assumed that partons are emitted and reabsorbed from the hadronic blobs collinear to the hadronic momenta. Since in the hard subprocesses there are no soft parameters available all dimension full variables have to be scaled by the hard scale, the photon virtuality, Q^2 . Due to our supposition of $t_i \ll Q^2$ we have to calculate the subprocess amplitudes in the limit $t_i \rightarrow 0$. In this limit the parton momenta simplify to

$$\begin{aligned}k_a &= [(x_1 + \xi_1)\bar{p}_a^+, 0, \mathbf{0}_\perp], & k_b &= [0, (x_2 + \xi_2)\bar{p}_b^-, \mathbf{0}_\perp], \\ k_1 &= [(x_1 - \xi_1)\bar{p}_a^+, 0, \mathbf{0}_\perp], & k_2 &= [0, (x_2 - \xi_2)\bar{p}_b^-, \mathbf{0}_\perp].\end{aligned}\quad (9)$$

We see that the parton momenta attached to the upper vertex in Fig. 1 have large plus components whereas those emitted and reabsorbed from the lower vertex have large minus components. In terms of the parton momenta the virtual photon momentum is approximately given by

$$q_3 \simeq [2\xi_1\bar{p}_a^+, 2\xi_2\bar{p}_b^-, \mathbf{0}_\perp].\quad (10)$$

With the help of (5) and (7) one readily sees that we correctly have

$$q_3^2 \simeq Q^2.\quad (11)$$

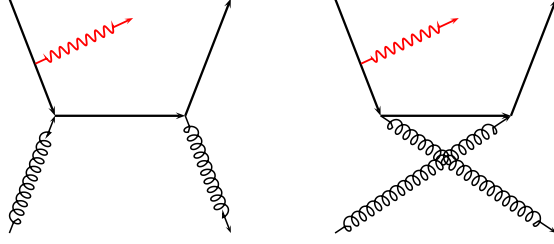


Figure 2: Typical leading order Feynman graphs for the subprocesses $q\bar{q} \rightarrow q\bar{q}\gamma^*$.

We are going to compute the subprocess amplitudes to leading-order of QCD and to leading-twist accuracy. The possible subprocesses are $q(\bar{q})g \rightarrow q(\bar{q})g\gamma^*$ and $qq(\bar{q}) \rightarrow qq(\bar{q})\gamma^*$. The subprocess $gg \rightarrow gg\gamma^*$ is suppressed by α_s and, hence, neglected. Typical leading order Feynman graphs for the relevant subprocesses are shown in Figs. 2 and 3. Obviously, the virtual photon is to be coupled to all quark lines. Since the parton helicities are not observed they have to be averaged over with some projector operator onto the hadronic state. Thus, in the following, we will deal with the amplitude for the subprocess $bc \rightarrow bc\gamma^*$ summed over the helicities, λ_b, λ_c , of the partons b and c which corresponds to the projector $p_\mu \gamma^\mu$ (being also the density matrix of unpolarized partons, when the imaginary part of the amplitude is considered by the use of the optical theorem):

$$\mathcal{H}_\nu^{bc} = \frac{1}{4} \sum_{\lambda_b \lambda_c} \mathcal{H}_{\lambda_b \lambda_c \nu, \lambda_b \lambda_c}^{bc}. \quad (12)$$

Since we are dealing with light quarks any quark-helicity-flip amplitude is zero. Nevertheless, the quarks or antiquarks emitted and reabsorbed from a hadronic vertex may have opposite helicities. Such configurations come from subprocesses like $q(+)\bar{q}(-) \rightarrow q(-)\bar{q}(+)\gamma^*$ or $q(+)\bar{q}(-) \rightarrow q(-)\bar{q}(+)\gamma^*$. In these cases the corresponding subprocess amplitudes are to be convoluted with transversity GPDs. Contributions of this type are neglected in this work. It is expected that for valence quarks this contribution is of about the same magnitude as the contribution from the valence-quark GPD H [9, 18]. The gluonic transversity GPDs do not contribute here since the corresponding subprocess amplitude vanishes for $t_i \rightarrow 0$. As our numerical analysis reveals, see Sect. 6, the dominant contribution to the processes of interest comes from the quark-gluon subprocess.

Straightforward calculations of the subprocesses reveal that only those for longitudinal polarization of the virtual photon ($\nu = 0$) are non-zero which is natural because of the similarity of the amplitude under consideration to the mesonic formfactors [19], where distribution amplitudes enter instead of GPDs. For the quark-gluon subprocess, see Fig. 2 for the relevant Feynman graphs, the

non-zero amplitude reads ⁴

$$\begin{aligned}
\mathcal{H}_0^{gg}(x_1, \xi_1, x_2, \xi_2) &= -16\pi \frac{\alpha_s(Q^2)}{N_c Q} \frac{1}{x_2 + \xi_2} \\
&\times \left\{ \left[\frac{1}{x_1 - \xi_1 - i\epsilon} - \frac{1}{x_1 + \xi_1 + i\epsilon} \right] \frac{1}{x_2 - \xi_2 + i\epsilon} \right. \\
&+ \frac{\xi_1}{x_1 + \xi_1 + i\epsilon} \frac{1}{(x_1 - \xi_1)(x_2 - \xi_2) + i\epsilon} \\
&\left. + \frac{\xi_1}{x_1 - \xi_1 - i\epsilon} \frac{1}{(x_1 + \xi_1)(x_2 - \xi_2) - i\epsilon} \right\}. \quad (13)
\end{aligned}$$

The momentum fraction x_2 as well as the skewness ξ_2 refer to the gluon. For the amplitude \mathcal{H}_0^{gg} one has to interchange x_1 and x_2 as well as ξ_1 and ξ_2 . In (13) N_c is the number of colors. The QCD coupling constant, α_s , is evaluated at the hard scale, the photon virtuality Q^2 , from the one-loop expression with $\Lambda_{\text{QCD}} = 220$ MeV and three flavors. Since the integral over the gluon's momentum fraction, x_2 , extends only from 0 to 1 as a consequence of the fact that the gluon GPD H is an even function of x , we have to consider only positive values of x_2 . Hence, the term $1/(x_2 + \xi_2)$ is not singular. The most singular integrals come from the terms

$$\frac{1}{(x_1 \pm \xi_1)(x_2 - \xi_2) \mp i\epsilon} \quad (14)$$

which is approximated by

$$\frac{1}{(x_1 \pm \xi_1)(x_2 - \xi_2) \mp i\epsilon} \simeq \frac{1}{x_1 \pm \xi_1 \mp i\epsilon} \frac{1}{x_2 - \xi_2 \mp i\epsilon}. \quad (15)$$

The recipe (15) can be justified to some extent by starting from the unphysical region with $|\xi_i| > 1$ and perform an analytic continuation [10] to the physical region where $|\xi_i| < 1$. The remaining problem is the different sign of ϵ for the continuation in s and s_1, s_2 . There are arguments [21] that the double spectral representation and a symmetric continuation in s_1, s_2 should be considered corresponding to positive ϵ . A special role is played by the inapplicability of the Steinmann relation because a virtual photon is involved in the process of interest. The interference with the electromagnetic contribution is especially interesting as only the real part of the DH amplitude is entering which is insensitive to the mentioned sign.

From (13) one sees that \mathcal{H}_0^{gg} possess the property

$$\mathcal{H}_0^{gg}(-x_1, \xi_1, x_2, \xi_2) = \mathcal{H}_0^{gg}(x_1, \xi_1, x_2, \xi_2). \quad (16)$$

⁴In addition to the momentum-space Feynman expressions there is a factor $1/\sqrt{x_1^2 - \xi_1^2}$ coming from the initial integration over k^- :

$$\frac{d\bar{k}^-}{\sqrt{4k_a^- k_1^-}} = \frac{dx_1}{\sqrt{x_1^2 - \xi_1^2}}$$

and, as a consequence of the use of light-cone gauge, a factor $1/[(x_2 + \xi_2)(x_2 - \xi_2 + i\epsilon)]$ arising from converting the gluon field, A_μ , appearing in the perturbative calculation, into the gluon field strength tensor, $G_{\mu\nu}$, in terms of which the gluonic GPDs are defined [2, 20]. The latter factor is absorbed in the subprocess amplitudes.

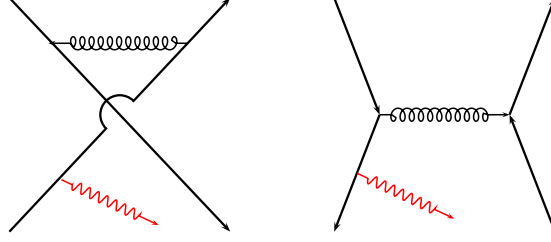


Figure 3: Typical leading order Feynman graphs for the subprocess $qq \rightarrow qq\gamma^*$.

The $qq \rightarrow qq\gamma^*$ subprocess amplitude is to be computed analogously from the leading-order Feynman graphs of the type shown on the left-hand side of Fig. 3:

$$\mathcal{H}_0^{qq}(x_1, \xi_1, x_2, \xi_2) = -16\pi \frac{\alpha_s(Q^2)}{N_c Q} \left\{ \frac{1}{(x_1 - \xi_1)(x_2 + \xi_2) - i\epsilon} - \frac{1}{(x_1 + \xi_1)(x_2 - \xi_2) - i\epsilon} \right\}. \quad (17)$$

The singular integrals are regularized according to Eq. (15). From (17) the following symmetry properties are evident

$$\begin{aligned} \mathcal{H}_0^{qq}(-x_1, \xi_1, -x_2, \xi_2) &= -\mathcal{H}_0^{qq}(x_1, \xi_1, x_2, \xi_2), \\ \mathcal{H}_0^{qq}(-x_1, \xi_1, x_2, \xi_2) &= -\mathcal{H}_0^{qq}(x_1, \xi_1, -x_2, \xi_2) \\ &= -16\pi \frac{\alpha_s(Q^2)}{N_c Q} \left\{ \frac{1}{(x_1 - \xi_1)(x_2 - \xi_2) + i\epsilon} - \frac{1}{(x_1 + \xi_1)(x_2 + \xi_2) + i\epsilon} \right\}. \end{aligned} \quad (18)$$

With the help of these symmetry relations one finds for the $\bar{q}\bar{q} \rightarrow \bar{q}\bar{q}\gamma^*$ amplitude

$$\mathcal{H}_0^{\bar{q}\bar{q}}(x_1, \xi_1, x_2, \xi_2) = \mathcal{H}_0^{qq}(-x_1, \xi_1, -x_2, \xi_2) = -\mathcal{H}_0^{qq}(x_1, \xi_1, x_2, \xi_2) \quad (19)$$

and for the $q\bar{q} (\bar{q}q)$ one which is to be calculated from the graphs shown on the right-hand side of Fig. 3,

$$\mathcal{H}_0^{q\bar{q}}(x_1, \xi_1, x_2, \xi_2) = \mathcal{H}_0^{\bar{q}q}(x_1, \xi_1, x_2, \xi_2) = \mathcal{H}_0^{qq}(x_1, \xi_1, -x_2, \xi_2). \quad (20)$$

As it becomes clear in the following section both the types of graphs shown in Fig. 3 lead to the same convolutions. Therefore, only the subprocess amplitude \mathcal{H}_0^{qq} , defined in Eq. (17), is to be taken into account because the $\bar{q}\bar{q}$, $q\bar{q}$ and $\bar{q}q$ amplitudes are contained in the convolution of \mathcal{H}_0^{qq} with a relevant GPD implying integrations over x_i from -1 to 1.

4 The process amplitudes

In the kinematical domain of interest in the present work helicity non-flip vertices $A \rightarrow A$ and $B \rightarrow B$ (i.e $\mu_a = \mu_1$, $\mu_b = \mu_2$) dominate which, in the handbag

approach, are under control of the GPD H . For proton and antiproton H is strictly speaking the combination

$$H_{\text{eff}} = H - \frac{\xi_i^2}{1 - \xi_i^2} E. \quad (21)$$

Contributions from the other GPDs like \tilde{H} , E or from transversity GPDs are expected to be small according to experience with GPDs extracted from data on electroproduction of vector mesons [22, 23]. Hence, we approximate H_{eff} by H . The full process amplitudes are given by the convolution⁵

$$\begin{aligned} \mathcal{M}_{\mu_a \mu_b \nu, \mu_a \mu_b}^{AB} &= e_0 \sqrt{1 - \xi_1^2} \sqrt{1 - \xi_2^2} \sum_{a=u,d,s} e_a \sum_{b,c} \int dx_1 dx_2 \\ &\times H_A^b(x_1, \xi_1, t_1) H_B^c(x_2, \xi_2, t_2) \mathcal{H}_0^{bc}(x_1, \xi_1, x_2, \xi_2) \end{aligned} \quad (22)$$

where b and c are either a quark of flavor a or a gluon, $H_A^b(x_1, \xi_1, t_1)$ ($H_B^c(x_2, \xi_2, t_2)$) is a quark or gluon GPD of the hadron A (B). The variable $x_1(x_2)$ is the average momentum fraction at the vertex $A \rightarrow A$ ($B \rightarrow B$). The positron charge is denoted by e_0 and e_a the charge of the quark in units of e_0 . Last not least, \mathcal{H}_0^{bc} is the subprocess amplitude defined in Eq. (12).

Next, we are going to discuss the amplitude (22) in combination with the subprocess amplitudes (13) and (17). With the help of (16) one can simplify the quark-gluon contribution to the amplitude (22):

$$\begin{aligned} \int_{-1}^1 dx_1 \int_0^1 dx_2 H_A^a(x_1, \xi_1, t_1) H_B^g(x_2, \xi_2, t_2) \mathcal{H}_{0a}^{gg}(x_1, \xi_1, x_2, \xi_2) = \\ \int_0^1 dx_1 \int_0^1 dx_2 \left[H_A^a(x_1, \xi_1, t_1) + H_A^a(-x_1, \xi_1, t_1) \right] \\ \times H_B^g(x_2, \xi_2, t_2) \mathcal{H}_{0a}^{gg}(x_1, \xi_1, x_2, \xi_2) \end{aligned} \quad (23)$$

and analogously for the gluon-quark contribution. For the quark GPDs the combinations ($j = A, B$)

$$H_j^{a(\pm)}(x, \xi, t) = H_j^a(x, \xi, t) \mp H_j^a(-x, \xi, t) \quad (24)$$

are even and odd under the replacement of x by $-x$:

$$H_j^{a(\pm)}(-x, \xi, t) = \mp H_j^{a(\pm)}(x, \xi, t). \quad (25)$$

Because of

$$H_j^{\bar{a}}(x, \xi, t) = -H_j^a(-x, \xi, t) \quad (26)$$

it is obvious that the plus combination in (24) which corresponds to the exchange of a charge conjugation even object in the t -channel, refers to a sea contribution whereas the minus one, corresponding to charge conjugation odd, is a valence-quark contribution [24].

For the quark-quark subprocess we have to take care of charge-conjugation invariance. Since the photon in the final state has $C = -1$, we need at one of

⁵For a pion vertex the factor $\sqrt{1 - \xi_i^2}$ does not appear.

the hadron vertices in Fig. 1 $C = -1$ and at the other one $C = +1$. In other words we have to consider the GPD products $H_A^{a(\pm)}(x_1, \xi_1, t_1) H_B^{a(\mp)}(x_2, \xi_2, t_2)$. The corresponding integral reads (dropping for a moment the arguments except of x_i , for convenience)

$$I = \int_{-1}^1 dx_1 \int_{-1}^1 dx_2 \left[H_A^{a(-)}(x_1) H_B^{a(+)}(x_2) + H_A^{a(+)}(x_1) H_B^{a(-)}(x_2) \right] \mathcal{H}_{0a}^{qq}(x_1, x_2). \quad (27)$$

The symmetry relation (25) allows to write this integral as

$$I = \int_0^1 dx_1 \int_0^1 dx_2 \left\{ \left[H_A^{a(-)}(x_1) H_B^{a(+)}(x_2) + H_A^{a(+)}(x_1) H_B^{a(-)}(x_2) \right] \times \left[\mathcal{H}_0^{qq}(x_1, x_2) - \mathcal{H}_0^{qq}(-x_1, -x_2) \right] + \left[H_A^{a(-)}(x_1) H_B^{a(+)}(x_2) - H_A^{a(+)}(x_1) H_B^{a(-)}(x_2) \right] \times \left[\mathcal{H}_0^{qq}(-x_1, x_2) - \mathcal{H}_0^{qq}(x_1, -x_2) \right] \right\}. \quad (28)$$

Using (26), one can further show that

$$\begin{aligned} H_A^{a(-)}(x_1) H_B^{a(+)}(x_2) + H_A^{a(+)}(x_1) H_B^{a(-)}(x_2) &= \\ &= 2H_A^a(x_1) H_B^a(x_2) - 2H_A^{\bar{a}}(x_1) H_B^{\bar{a}}(x_2), \\ H_A^{a(-)}(x_1) H_B^{a(+)}(x_2) - H_A^{a(+)}(x_1) H_B^{a(-)}(x_2) &= \\ &= 2H_A^a(x_1) H_B^{\bar{a}}(x_2) - 2H_A^{\bar{a}}(x_1) H_B^a(x_2). \end{aligned} \quad (29)$$

We see that the first combination of the GPDs refers to quark-quark and antiquark-antiquark scattering, i.e. it corresponds to Feynman graphs of the type shown on the left-hand side of Fig. 3 whereas the second combination represents quark-antiquark and antiquark-quark scattering (corresponding to graphs of the type shown on the right-hand side of Fig. 3). Thus, only the type of graphs shown on the left-hand side of Fig. 3 is to be taken into account. Quark-antiquark graphs, shown on the right-hand side of this figure, are already included because of the integrations from -1 to 1.

Putting all together what we have just discussed the amplitude (22) can be cast into the form

$$\begin{aligned} \mathcal{M}_{\mu_a \mu_b 0, \mu_a \mu_b}^{AB} &= e_0 \sqrt{1 - \xi_1^2} \sqrt{1 - \xi_2^2} \sum_a e_a \int_0^1 dx_1 \int_0^1 dx_2 \\ &\times \left\{ \left[H_A^{a(-)}(x_1, \xi_1, t_1) H_B^g(x_2, \xi_2, t_2) \mathcal{H}_0^{gg}(x_1, \xi_1, x_2, \xi_2) \right. \right. \\ &\quad \left. \left. + H_A^g(x_1, \xi_1, t_1) H_B^{a(-)}(x_2, \xi_2, t_2) \mathcal{H}_0^{gg}(x_2, \xi_2, x_1, \xi_1) \right] \right. \\ &+ 2 \left[H_A^a(x_1, \xi_1, t_1) H_B^a(x_2, \xi_2, t_2) - H_A^{\bar{a}}(x_1, \xi_1, t_1) H_B^{\bar{a}}(x_2, \xi_2, t_2) \right] \\ &\times \mathcal{H}_0^{qq}(x_1, \xi_1, x_2, \xi_2) \\ &+ 2 \left[H_A^a(x_1, \xi_1, t_1) H_B^{\bar{a}}(x_2, \xi_2, t_2) - H_A^{\bar{a}}(x_1, \xi_1, t_1) H_B^a(x_2, \xi_2, t_2) \right] \\ &\times \mathcal{H}_0^{qq}(-x_1, \xi_1, x_2, \xi_2) \left. \right\}. \end{aligned} \quad (30)$$

There are four amplitudes for proton-proton and proton-antiproton collisions for the helicities $\mu_a = \pm 1/2$ and $\mu_b = \pm 1/2$, for pion-proton collisions only two. Evidently these amplitudes are the same, there is only one independent amplitude for each process

$$\mathcal{M}^{pp(\bar{p})} = \mathcal{M}_{++0,++}^{pp(\bar{p})}. \quad (31)$$

and analogously for pion-proton scattering.

5 The electromagnetic lepton-pair production

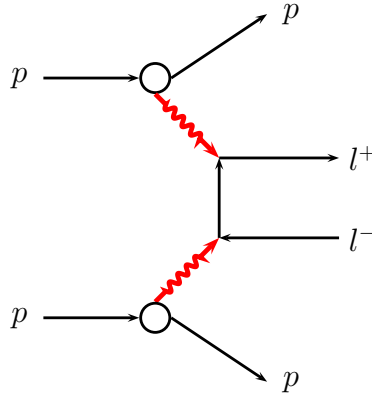


Figure 4: Graph for the electromagnetic lepton-pair production in exclusive proton-proton collisions. To leading-order there is a second graph with the lepton lines crossed.

At small t_i , the helicity amplitudes for the electromagnetic lepton-pair generation in proton-proton collisions read (remember the sum of the lepton and antilepton helicity is zero)

$$\begin{aligned} \mathcal{M}_{\mu_a \mu_b 0, \mu_a \mu_b}^{\text{elm}} &= \frac{16\pi^2 \alpha_{\text{em}}^2}{t_1 t_2} \frac{G_M(t_1) G_M(t_2)}{\sqrt{(s-s_1)(s-s_2)}} \frac{E_q s^{3/2} (Q^2 - s_1)(s - s_1)}{s_1^3 s_2} \\ &\times \left[Q^2 s_1 \sqrt{s} \cos \theta_q \right. \\ &+ \left. E_q (1 - \sin \theta_q \cos \phi_q) (Q^2 s (1 - \cos \theta_q) - s_1^2 (1 + \cos \theta_q)) \right] \\ &+ \mathcal{O}(t_1, t_2). \end{aligned} \quad (32)$$

The positively charged lepton momentum is defined as

$$q = E_q (1, \sin \theta_q \cos \phi_q, \sin \theta_q \sin \phi_q, \cos \theta_q). \quad (33)$$

Similar contributions exist for proton-antiproton and meson-proton collisions.

The interference between the electromagnetic and the double-handbag contributions is particularly interesting: It is linear in the GPDs and contains only the real part of the strong amplitude independent on the regularization scheme exploited. As the electromagnetic and strong amplitudes corresponds to a different C-parity of the lepton pair, the interference term is antisymmetric with

respect to the interchange of the leptons, in complete analogy to TVCS case [13]. As a consequence the interference term becomes zero if it is integrated over the entire range of dilepton angles.

The interference term may be used as a probe of the handbag contribution on top of the electromagnetic one. The theoretically cleanest way would be to consider the differential asymmetry for fixed momenta of the lepton pair [25]:

$$A = \frac{d\sigma(e^+(p_1)e^-(p_2)) - d\sigma(e^+(p_2)e^-(p_1))}{d\sigma(e^+(p_1)e^-(p_2)) + d\sigma(e^+(p_2)e^-(p_1))}. \quad (34)$$

However, this requires a very high accuracy which can be hardly achieved because of the smallness of the cross-section. One can also perform integration for polar and/or azimuthal angles, like in TVCS [13], where the spin-dependent and spin-independent terms have different symmetry properties with respect to the reflection of angles. This, in turn, would also require a very good acceptance. Another method to measure the interference term will be discussed in Sect. 6.1.

6 Results

6.1 Proton-proton collisions

For the case of proton-proton collisions we omit the particle labels A, B at the GPDs for convenience and use the familiar notation H^a for quarks of flavor a and H^g for gluons. For predictions of the corresponding cross section for lepton-pair production we can make use of the GPDs extracted from nucleon form factors [26] and from electroproduction of vector mesons [22]. In the analysis of the nucleon form factors the GPDs H and E for valence quarks can be extracted for a given parameterization of the zero-skewness GPDs as a product of the forward limit, the parton densities in the case of H , and an exponential in t with a profile function assumed to be

$$f_a(x) = \alpha'_a(1-x)^3 \ln(1/x) + B_a(1-x)^3 + A_ax(1-x)^2. \quad (35)$$

The parameters α'_a , B_a and A_a are fixed from a fit to the nucleon form factor data. The skewness dependence of the GPDs is generated from the double-distribution ansatz [27] whereby the double distribution is assumed to be a product of the zero-skewness GPD and an appropriate weight function. The gluon and sea quark GPDs at zero skewness are parameterized analogously with a small $-t$, small x approximation of the profile function (35)

$$f_a(x) \simeq \alpha'_a \ln(1/x) + B_a. \quad (36)$$

For the sea quark GPDs we adopt a result from CTEQ [28] it is assumed that

$$H^{\bar{u}} = H^{\bar{d}} = \kappa_s H^s = \kappa_s H^{\bar{s}} \quad (37)$$

with the flavor-symmetry breaking factor

$$\kappa_s = 1 + 0.68/(1 + 0.52 \ln(Q^2/Q_0^2)). \quad (38)$$

With the assumption $H^s = H^{\bar{s}}$ the strange-quark contributions to the amplitude (22) cancel. The initial scale, Q_0 , for the GPDs is taken as 2 GeV. The

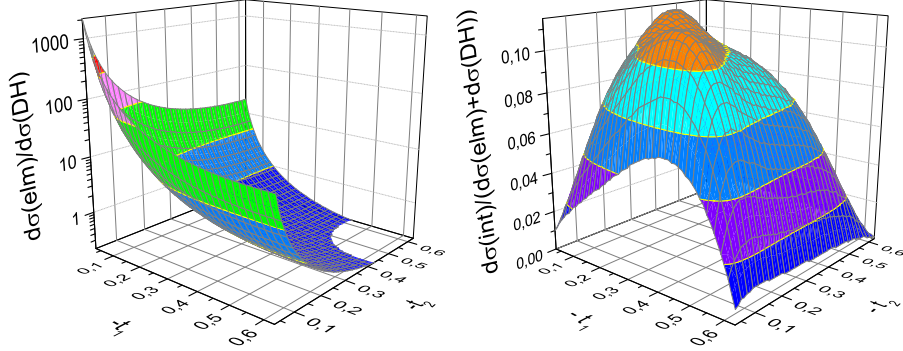


Figure 5: Left: The ratio of the electromagnetic and DH cross sections for $pp \rightarrow pp l^+ l^-$ versus t_1 and t_2 (in GeV^2) at a kinematics typical for NICA ($\sqrt{s} = 24 \text{ GeV}$, $Q^2 = 3 \text{ GeV}^2$).

Figure 6: Right: The ratio of the interference cross section and the sum of the electromagnetic and DH contributions at the same kinematics as in Fig. 5. The decay angle θ^* is only integrated from 0 to $\pi/2$.

profile functions for the gluon and sea-quark GPDs are obtained from fits to the available HERA data on ρ^0 and ϕ electroproduction [29, 30]. The parameters of the GPDs can be found in [22]. These GPDs have been used to predict DVCS [31] and ω electroproduction [32]; good agreement with experiment is achieved. This strengthens our confidence in the reliability of the predictions for lepton-pair production. Since in the present paper we are merely interested in values of Q^2 close to the initial scale of 4 GeV^2 evolution of the GPDs plays only a minor role and we simply use their Q^2 -dependence given in [22]. For Q^2 substantially larger than Q_0^2 evolution is to be taken into account correctly which, in principle, can be done with the Vinnikov code [33].

The relative strength of the electromagnetic and the DH contributions are displayed in Fig. 5 for a typical kinematics accessible at the NICA accelerator. Shown is the ratio of $pp \rightarrow pp l^+ l^-$ cross section integrated over the full range of dilepton angles (see Eq. (58) in App. A)

$$\frac{d\sigma(pp \rightarrow pp l^+ l^-)}{dt_1 dt_2 dQ^2} = \frac{1}{3(4\pi)^5} \frac{\alpha_{\text{em}}}{s^2 Q^2} \int \frac{ds_1 ds_2}{\sqrt{-\Delta_4}} |\mathcal{M}|^2. \quad (39)$$

where \mathcal{M} is either the electromagnetic amplitude (32) or the DH one, Eq. (30). Since it is integrated over the dilepton angles there is no interference between the two contributions. Due to the singular behavior of the electromagnetic amplitude (32) for $t_i \rightarrow 0$ it dominates the process at small t_i . Only for $-t_i$ larger than about 0.4 GeV^2 the DH contribution takes the lead. The cross sections (39) are symmetric in t_1 and t_2 .

As mentioned in Sect. 5 the interference between the electromagnetic and the double-handbag contribution is interesting since it is proportional to the real part of the double-handbag amplitude

$$d\sigma^{\text{int}} \propto \mathcal{M}^{\text{elm}} \text{Re} \mathcal{M}^{pp}. \quad (40)$$

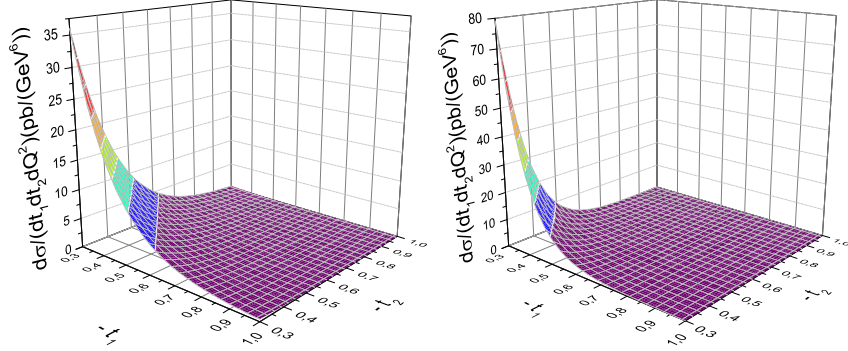


Figure 7: Left: The DH contribution to the $pp \rightarrow pp l^+ l^-$ cross section (in pb/ GeV⁶) versus t_1 and t_2 (in GeV²) at $\sqrt{s} = 24$ GeV and $Q^2 = 3$ GeV².

Figure 8: Right: The DH contribution to the $pp \rightarrow pp l^+ l^-$ cross section in pb/ GeV⁶ versus t_1 and t_2 (in GeV²) at a typical LHC kinematics: $\sqrt{s} = 13$ TeV and $Q^2 = 5$ GeV².

As above said the double-handbag amplitude is dominantly real and approximately proportional to the product $H^q H^g$ at $x_i = \xi_i$ even though the product is integrated over a certain range of the ξ_i implied in the integration over the s_i , see Eq. (7). As one may see from Fig. 6 the ratio of the interference cross section and the sum of the electromagnetic and the DH contributions is rather large, of the order of 0.1 at the NICA kinematics, and has two identical maxima at $(t_1, t_2) = (-0.13 \text{ GeV}^2, -0.37 \text{ GeV}^2)$ and $(-0.37 \text{ GeV}^2, -0.13 \text{ GeV}^2)$. In order to obtain a non-zero result for the interference term the photon decay angle θ^* (see App. A) is only integrated from 0 to $\pi/2$.

In Figs. 7 and 8 the differential cross section (39) for $pp \rightarrow pp l^+ l^-$ are shown at a typical kinematics accessible at NICA and at the LHC, respectively. The cross section is only shown for $-t_i$ larger than 0.3 GeV². Only the DH contribution is taken into account in this region; the electromagnetic contribution is here neglected. The DH contribution is strongly forward peaked but, for $-t_i \leq 0.3 \text{ GeV}^2$, it is overwhelmed by the electromagnetic lepton-pair generation, see Fig. 5. We stress that our numerical studies reveal the dominance of the quark-gluon subprocess, the quark-quark contribution is almost negligible. In fact, $|\mathcal{M}^{qq}|/|\mathcal{M}^{qg}| \leq 0.1$ for the entire kinematical region explored by us. It is also important to realize that the main contribution of the quark-gluon subprocess is generated from the imaginary parts of the two vertex functions. Thus, the subprocess amplitude is dominantly real and approximately proportional to the product $H^q H^g$ at $x_i = \xi_i$. Since $H^g(\xi_i, \xi_i, t_i)$ strongly increases with decreasing skewness the cross section is rising with s at fixed Q^2 (see (7)).

6.2 Proton-antiproton collisions

Let us now turn to dilepton production in proton-antiproton collisions which can be measured at the future PANDA experiment at the FAIR facility. The antiproton GPDs from the lower vertex in Eq. (30) are related to the proton

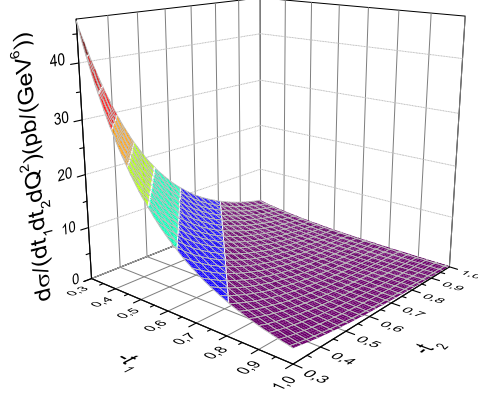


Figure 9: The $p\bar{p} \rightarrow p\bar{p}l^+l^-$ cross section in pb/GeV^6 versus t_1 and t_2 (in GeV^2) at a typical FAIR kinematics: $s = 30 \text{ GeV}^2$, $Q^2 = 3 \text{ GeV}^2$.

ones by

$$H_{\bar{p}}^{\bar{a}}(x_2, \xi_2, t_2) = H^a(x_2, \xi_2, t_2), \quad H_{\bar{p}}^g(x_2, \xi_2, t_2) = H^g(x_2, \xi_2, t_2). \quad (41)$$

From these relations it is evident that the contributions from the quark-gluon subprocess is the same for proton-proton and proton-antiproton collisions while the role of the last two terms in (30) are interchanged: The second last term now refers to quark-antiquark scattering (see the right-hand side of Fig. 3) whereas the last one represents quark-quark and antiquark-antiquark scattering (see left-hand side of Fig. 3). These considerations make it clear that the cross section for proton-proton and proton-antiproton collisions are identical for the same kinematics especially since the quark-gluon contribution dominates over the quark-quark one. In Fig. 9 the cross section of the process of interest is displayed for a typical FAIR kinematics.

6.3 Pion-proton collisions

The last process we want to discuss briefly is $\pi p \rightarrow \pi p l^+ l^-$. Since the quark-quark contribution to this process has already been discussed in [19] we focus our interest to the quark-gluon contribution. Applying charge conjugation symmetry to the pion GPDs one finds [34]

$$H_{\pi^+}^a(x_1, \xi_1, t_1) = -H_{\pi^-}^a(-x_1, \xi_1, t_1). \quad (42)$$

In combination with isospin symmetry this leads to (for convenience the variables ξ_1 and t_1 are dropped for a moment)

$$\begin{aligned} H_{\pi^+}^u(x_1) &= -H_{\pi^+}^d(-x_1) = H_{\pi^+}^{\bar{d}}(x_1), \\ H_{\pi^-}^d(x_1) &= -H_{\pi^-}^u(-x_1) = H_{\pi^-}^{\bar{u}}(x_1). \end{aligned} \quad (43)$$

Hence,

$$H_{\pi^\pm}^u(x_1) = H_{\pi^\mp}^d(x_1). \quad (44)$$

Inspection of the amplitude (30) reveals that for the quark-gluon contribution the sums of the pion's and proton's quark GPDs occur. Each GPD is to be

multiplied by the corresponding quark charge. Because of

$$\begin{aligned} H_{\pi^-}^{u(-)}(x_1) &= H_{\pi^-}^u(x_1) + H_{\pi^-}^u(-x_1) = H_{\pi^-}^u(x_1) - H_{\pi^-}^{\bar{u}}(x_1) \\ &= H_{\pi^-}^u(x_1) - H_{\pi^-}^d(x_1) \end{aligned} \quad (45)$$

and analogously for $H_{\pi^-}^{d(-)}$, the sum of the pion's quark GPD simplifies to

$$\sum_a e_a H_{\pi^-}^{a(-)}(x_1) = H_{\pi^-}^u(x_1) - H_{\pi^-}^d(x_2) \quad (46)$$

where we made the plausible assumption $H_{\pi^-}^s(x_1) = H_{\pi^-}^{\bar{s}}(x_1)$. The quark-gluon contribution to the $\pi^- p$ amplitude then reads

$$\begin{aligned} \mathcal{M}^{\pi^- p} &= e_0 \sqrt{1 - \xi_2^2} \int_0^1 dx_1 \int_0^1 dx_2 \\ &\times \left\{ \left[H_{\pi^-}^u(x_1, \xi_1, t_1) - H_{\pi^-}^d(x_1, \xi_1, t_1) \right] H^g(x_2, \xi_2, t_2) \mathcal{H}_0^{qg}(x_1, \xi_1, x_2, \xi_2) \right. \\ &\quad \left. + H_{\pi^-}^g(x_1, \xi_1, t_1) \sum_a e_a H^{av}(x_2, \xi_2, t_2) \mathcal{H}_0^{qg}(x_2, \xi_2, x_1, \xi_1) \right\}. \end{aligned} \quad (47)$$

Thus, only the valence-quark proton GPDs

$$H^{av}(x_2, \xi_2, t_2) = H^a(x_2, \xi_2, t_2) - H^{\bar{a}}(x_2, \xi_2, t_2) \quad (48)$$

contribute. As in the other cases we investigated, the quark-gluon contribution is much larger than the quark-quark ones. An analogous result is found for the case of a π^+ beam. The generalization of this amplitude to the case of a Kaon beam is straightforward. Our process $\pi p \rightarrow \pi p l^+ l^-$ as well as $K p \rightarrow K p l^+ l^-$ can be measured at the future J-PARC accelerator. The measurement of these cross section give in principle access to the pion and Kaon GPDs. In so far the dynamics can be explored in greater detail than with the pion (or Kaon) induced exclusive Drell-Yan process [35, 36].

Because of the very limited knowledge of the pion GPDs we refrain from giving numerical estimates of the $\pi p \rightarrow \pi p l^+ l^-$ cross section.

7 Summary

We have investigated lepton-pair production in exclusive hadronic collisions within the handbag approach. It is assumed that the process amplitude factorizes in a hard partonic subprocess, $q\bar{q}(\bar{q}) \rightarrow q\bar{q}(\bar{q}) l^+ l^-$ and $q\bar{q} \rightarrow q\bar{q} l^+ l^-$, and soft hadronic matrix elements, $A \rightarrow A$ and $B \rightarrow B$, which are parameterized as GPDs. We have derived the amplitudes for this DH mechanism and discussed their properties. The dominant contribution comes from the GPD H in combination with the $q\bar{q} \rightarrow q\bar{q} \gamma^*$ subprocess. The $q\bar{q}(\bar{q}) \rightarrow q\bar{q}(\bar{q}) \gamma^*$ subprocess is also considered but its contribution is much smaller than that from the quark-gluon one. We have made predictions for the lepton-pair production in exclusive proton-proton and proton-antiproton collisions for kinematics accessible at NICA, LHC and FAIR.

The DH contribution competes with the purely electromagnetic lepton-pair production. The latter one is singular for $t_i \rightarrow 0$ and, hence, dominates for

$-t_i \lesssim 0.4 \text{ GeV}^2$. The interference between the two contributions is interesting because it is proportional to the real part of the DH amplitude which itself is approximately given by the product $H^q H^g$ at $x_i = \xi_i$. However, the interference term is zero if it is integrated over the entire range of dilepton angles.

We have also briefly examined lepton-pair production in exclusive pion-proton collisions. Measurements of this cross section which is in principle possible at the future J-PARC accelerator, would give access to the pion GPDs. The generalization to the corresponding process with a Kaon beam is straightforward.

Acknowledgements We are grateful to Helmut Koch for information about the measurability of $p\bar{p} \rightarrow p\bar{p}l^+l^-$ with the PANDA experiment.

A Phase space and the decay of the virtual photon

Denoting the lepton momenta by q and q' and inserting the relation

$$1 = \delta^{(4)}(p_a + p_b - q_1 - q_2 - q_3) d^3q_3 dE_3, \quad (49)$$

one can write the four-particle phase space as

$$dLips_4(p_a p_b \rightarrow q_1 q_2 q q') = dLips_3(p_a p_b \rightarrow q_1 q_2 q_3) \frac{2E_3 dE_3}{2\pi} dLips_2(q_3 \rightarrow q q'). \quad (50)$$

In terms of the invariants the three-particle phase space reads

$$dLips_3(p_a p_b \rightarrow q_1 q_2 q_3) = \frac{1}{(2\pi)^5} \frac{\pi}{16s} \frac{dt_1 dt_2 s_1 s_2}{\sqrt{-\Delta_4}} \quad (51)$$

where in the massless case [16]

$$\begin{aligned} \Delta_4 = & \frac{1}{16} \left\{ sQ^2 \left[s(Q^2 - 2t_1 - 2t_2) - 2(s_1 s_2 + 2t_1 t_2 - t_1 s_1 - t_2 s_2) \right] \right. \\ & + t_1^2 (s - s_1)^2 + t_2^2 (s - s_2)^2 + 2s_1 s_2 t_1 (s - s_1) \\ & \left. + 2s_1 s_2 t_2 (s - s_2) - 2t_1 t_2 s (s - s_1 - s_2) + s_1 s_2 (s_1 s_2 + 2t_1 t_2) \right\}. \end{aligned} \quad (52)$$

The decay of the virtual photon is considered in its rest frame, Σ^* . Then

$$dQ^2 = 2E_3 dE_3 \quad (53)$$

and

$$dLips_2(q_3^* \rightarrow q^* q'^*) = \frac{1}{32\pi^2} d\cos\theta^* d\phi^*. \quad (54)$$

The angles θ^* and ϕ^* are the decay angles in the frame Σ^* . The amplitude for the process $AB \rightarrow ABll$ is given by

$$T_{\mu_a \mu_b \lambda - \lambda, \mu_a \mu_b}^{AB} = \frac{e_0}{Q} \bar{u}(q, \lambda) \epsilon(\nu) \cdot \gamma v(q', -\lambda) \mathcal{M}_{\mu_a \mu_b 0, \mu_a \mu_b}^{AB}. \quad (55)$$

Summing the square of the amplitude T over the final state helicities and averaging those in the initial state we arrive at

$$|T_L^{AB}|^2 = 2 \sin\theta^* \frac{e_0^2}{Q^2} |\mathcal{M}_{++0,++}^{AB}|^2. \quad (56)$$

The spin averaged cross section reads

$$d\sigma(AB \rightarrow ABll) = 4\pi \frac{\alpha_{\text{em}}}{sQ^2} dLips_4 \sin^2 \theta^* |\mathcal{M}_{++0,++}^{AB}|^2. \quad (57)$$

Using (50) and integrating over the decay angles of the virtual photon we arrive at the differential cross section

$$\frac{d\sigma(AB \rightarrow ABll)}{dt_1 dt_2 dQ^2} = \frac{1}{3(4\pi)^5} \frac{\alpha_{\text{em}}}{s^2 Q^2} \int \frac{ds_1 ds_2}{\sqrt{-\Delta_4}} |\mathcal{M}_{++0,++}^{AB}|^2. \quad (58)$$

References

- [1] X. D. Ji, Phys. Rev. D **55**, 7114 (1997) [hep-ph/9609381].
- [2] A. V. Radyushkin, Phys. Lett. B **385**, 333 (1996) [hep-ph/9605431].
- [3] J. C. Collins, L. Frankfurt and M. Strikman, Phys. Rev. D **56**, 2982 (1997) [hep-ph/9611433].
- [4] J. C. Collins and A. Freund, Phys. Rev. D **59**, 074009 (1999) [hep-ph/9801262].
- [5] A. V. Radyushkin, Phys. Rev. D **58**, 114008 (1998) [hep-ph/9803316].
- [6] M. Diehl, T. Feldmann, R. Jakob and P. Kroll, Eur. Phys. J. C **8**, 409 (1999) [hep-ph/9811253].
- [7] M. Diehl, T. Gousset, B. Pire and O. Teryaev, Phys. Rev. Lett. **81**, 1782 (1998) [hep-ph/9805380].
- [8] M. Defurne *et al.* [Jefferson Lab Hall A Collaboration], Phys. Rev. Lett. **117**, no. 26, 262001 (2016) [arXiv:1608.01003 [hep-ex]].
- [9] S. V. Goloskokov and P. Kroll, Eur. Phys. J. A **47**, 112 (2011) [arXiv:1106.4897 [hep-ph]].
- [10] O. V. Teryaev, hep-ph/0510031.
- [11] A. T. Goritschnig, P. Kroll and W. Schweiger, Eur. Phys. J. A **42**, 43 (2009) [arXiv:0905.2561 [hep-ph]].
- [12] S. Koffler, P. Kroll and W. Schweiger, Phys. Rev. D **91**, 054027 (2015) [arXiv:1412.5367 [hep-ph]].
- [13] E. R. Berger, M. Diehl and B. Pire, Eur. Phys. J. C **23**, 675 (2002) [hep-ph/0110062].
- [14] O. Grocholski, H. Moutarde, B. Pire, P. Sznajder and J. Wagner, arXiv:1912.09853 [hep-ph].
- [15] A. Cisek, W. Schafer and A. Szczurek, Int. J. Mod. Phys. A **26**, 636 (2011).
- [16] E. Byckling and K. Kajantie, Particle Kinematics, Wiley (1972).
- [17] X. D. Ji, J. Phys. G **24**, 1181 (1998) [hep-ph/9807358].

- [18] S. V. Goloskokov and P. Kroll, Eur. Phys. J. C **74**, 2725 (2014) [arXiv:1310.1472 [hep-ph]].
- [19] A. A. Pivovarov and O. V. Teryaev, XXII International Baldin Seminar on High Energy Physics Problems JINR, Dubna, Russia, September 2014
- [20] J. B. Kogut and D. E. Soper, Phys. Rev. D **1**, 2901 (1970).
- [21] O. V. Teryaev, “Analytic Properties of DPE Amplitudes or Collinear Factorisation for Central Exclusive Production,” Contribution to EDS09 <https://inspirehep.net/files/9e04c8d6d0e1bd7c99858c8e23cd1f12>.
- [22] S. V. Goloskokov and P. Kroll, Eur. Phys. J. C **53**, 367 (2008) [arXiv:0708.3569 [hep-ph]].
- [23] P. Kroll, EPJ Web Conf. **85**, 01005 (2015) [arXiv:1410.4450 [hep-ph]].
- [24] M. Diehl, Phys. Rept. **388**, 41 (2003) [hep-ph/0307382].
- [25] A. A. Pivovarov and O. V. Teryaev, AIP Conf. Proc. **1654** (2015) no.1, 070008
- [26] M. Diehl and P. Kroll, Eur. Phys. J. C **73**, no. 4, 2397 (2013) [arXiv:1302.4604 [hep-ph]].
- [27] I. V. Musatov and A. V. Radyushkin, Phys. Rev. D **61** (2000) 074027 [hep-ph/9905376].
- [28] J. Pumplin, D. R. Stump, J. Huston, H. L. Lai, P. M. Nadolsky and W. K. Tung, JHEP **0207**, 012 (2002) [hep-ph/0201195].
- [29] C. Adloff *et al.* [H1 Collaboration], Eur. Phys. J. C **13**, 371 (2000) [hep-ex/9902019].
- [30] S. Chekanov *et al.* [ZEUS Collaboration], Nucl. Phys. B **718**, 3 (2005) [hep-ex/0504010].
- [31] P. Kroll, H. Moutarde and F. Sabatie, Eur. Phys. J. C **73**, no. 1, 2278 (2013) [arXiv:1210.6975 [hep-ph]].
- [32] S. V. Goloskokov and P. Kroll, Eur. Phys. J. A **50**, no. 9, 146 (2014) [arXiv:1407.1141 [hep-ph]].
- [33] A. V. Vinnikov, hep-ph/0604248.
- [34] C. Mezrag, H. Moutarde, J. Rodríguez-Quintero and F. Sabatié, arXiv:1406.7425 [hep-ph].
- [35] S. V. Goloskokov and P. Kroll, Phys. Lett. B **748**, 323 (2015). [arXiv:1506.04619 [hep-ph]].
- [36] T. Sawada, W. C. Chang, S. Kumano, J. C. Peng, S. Sawada and K. Tanaka, Phys. Rev. D **93**, no. 11, 114034 (2016) [arXiv:1605.00364 [nucl-ex]].